Aquaporin-1 Water Channel Expression in Human Kidney

ARVID B. MAUNSBACH,* DAVID MARPLES,† EDWARD CHIN,‡ GANG NING,* CAROLYN BONDY,‡ PETER AGRE,§ and SØREN NIELSEN*

**Department of Cell Biology, Institute of Anatomy, University of Aarhus, Aarhus, Denmark; †Department of Physiology, University of Leeds, Leeds, United Kingdom; ‡National Institute of Child Health and Human Development, National Institutes of Health, Bethesda, Maryland; §Departments of Medicine and Biological Chemistry, Johns Hopkins University Medical School, Baltimore, Maryland.*

Abstract. The pattern of aquaporin-1 water channel protein (AQP1) expression in the human kidney was analyzed by immunocytochemistry using semi-thin and optimized high-resolution immunoelectron microscopy based on freeze-substituted and Lowicryl HM20 embedded tissue. In addition, *in situ* hybridization was used to determine AQP1 mRNA distribution. Immunoblots revealed a 28-kd band and a 35- to 45-kd band corresponding to unglycosylated and glycosylated AQP1. Glomerular capillary endothelium exhibited extensive AQP1 labeling, whereas glomerular podocytes and Bowman's capsule epithelium were unlabeled. AQP1 was localized in the proximal tubule, including the neck region directly connected to the glomerulus. However, there was a marked difference in the level of expression between cross-sections of the convoluted part and the proximal straight tubules, the latter displaying the most intense labeling. AQP1 labeling continued uninterrupted from the proximal straight tubule into descending thin limbs in outer medulla. Abrupt transitions from heavily labeled to unlabeled segments of thin limbs were observed, primarily in the inner medulla. This may represent the transition from the water-permeable thin descending limb to the water-impermeable thin ascending limb. In addition, heavy labeling of fenestrated endothelium was also observed in peritubular capillaries in cortex, outer medulla, and inner medulla. Immunolabeling controls were negative. *In situ* hybridization documented a marked difference in AQP1 mRNA levels within the proximal tubule, with the greatest AQP1 mRNA expression in straight proximal tubules. Glomeruli also showed marked signals, and descending thin limbs exhibited extensive expression in exact concordance with the immunocytochemical results. It was concluded that: (*1*) AQP1 is present in all proximal tubule segments, including segment 1 and the neck region, but there is a pronounced difference in expression levels with respect to both protein and mRNA levels; (*2*) AQP1 labeling is observed in the endothelium of fenestrated peritubular capillaries, as well as fenestrated glomerular capillaries; (*3*) AQP1 labeling continues directly from proximal tubules to descending thin limbs; and (*4*) abrupt transitions from labeled to unlabeled thin limb epithelium are noted. (J Am Soc Nephrol 8: 1–14, 1997)

The aim of the study presented here was to investigate the localization of aquaporin-1 water channel protein (AQP1) in the human kidney and thereby to obtain information about the potential role of this water channel in human renal physiology. Particular emphasis has been placed on a comparison with the distribution of AQP1 in the rat kidney, where detailed studies have been performed (5,17,18,22; for recent reviews, see References 7 and 16). This seems particularly important because the architectural and ultrastructural organization of the human kidney—especially in the outer and inner medulla—is complex, and detailed electron microscopical analyses (4,15,24,25) have revealed ultrastructural characteristics that differ in many respects from the ultrastructural organization of the rat nephron (for reviews, see References 9, 12, 14, and 26). To achieve a precise cellular localization of AQP1 in the human kidney, immunoelectron microscopic analyses were performed using Lowicryl sections of cryosubstituted tissue, which retain antigenicity and give uniform labeling efficiency combined with optimal ultrastructural preservation. This allowed direct comparison of the expression of AQP1 from segment to segment, and from cell to cell. To further substantiate the expression of AQP1 in different nephron segments AQP1 mRNA was localized by *in situ* hybridization.

AQP1 is the first molecular water channel to have been identified (20,27) and its discovery has led to the characterization of a family of membrane water channels, the aquaporins (1,7,16). The cellular and subcellular localization of AQP1 in the rat kidney has been thoroughly examined by immunoperoxidase, immunofluorescence, and immunoelectron microscopy using cryosections and Lowicryl sections. AQP1 is expressed abundantly in the proximal tubule, although the initial portion of the proximal tubule exhibits substantially lower immunolabeling signals (18). The expression continues into descending thin limbs of both short loops and long loops in the renal medulla (17,18). There is an abrupt transition from labeled cells in the descending thin limb to unlabeled cells in the ascending thin limb, consistent with the water-permeability characteristics of thin limb segments (17,18). Thus, AQP1 has

Received July 16, 1996. Accepted August 22, 1996.
Correspondence to Dr. Arvid B. Maunsbach, Department of Cell Biology, Institute of Anatomy, University of Aarhus, DK-800 Aarhus C, Denmark.
1046-6673/0801-0001$03.00/0
Journal of the American Society of Nephrology

a distribution in concordance with the known water permeability of the nephron (17,18), with the exception of the initial portions of the proximal tubule. It remains to be established whether another aquaporin homologue is expressed at this site. Initial studies (5) have shown that AQP1 is expressed in the human proximal tubule. However, the exact localization pattern in the human nephron has not been determined.

In the rat, AQP1 is also present in plasma membranes of various secretory and reabsorptive epithelia (3,19) as well as in nonfenestrated endothelium of capillaries (19). The localization in capillary endothelium has also been characterized in the rat kidney, where AQP1 is expressed in descending vasa recta, a site at which mercurial chloride treatment of isolated perfused descending vasa recta revealed significant impairment in water permeability (12). These studies underscore the hypothesis that AQP1 plays a major role in transepithelial water movement at multiple sites.

The importance of examining the expression pattern of AQP1 in the human kidney is further accentuated by the recent report that rare human individuals apparently lacking AQP1 do not show major clinical abnormalities (21). Thus, it is important to determine the precise expression pattern along the human nephron to allow correlations between the presence (or absence) of AQP1 and water transport in the different segments of the human nephron. Moreover, the recent demonstration of aquaporin excretion in human urine (6,21) and the discussion of a potential use of this for diagnosing urinary concentrating defects (8) also emphasize the need to characterize the localization of aquaporins in the human kidney tubule to enable interpretation of such information.

Methods

Preparation of Membrane Vesicles from Human Kidney

Cortex, outer medulla, and inner medulla were dissected from surgical specimens of human kidney, minced finely, and homogenized in dissecting buffer (0.3 M sucrose, 25 mM imidazole, 1 mM EDTA, pH 7.2, and containing the following protease inhibitors: 8.5 μM leupeptin, 1 mM phenylmethyl sulfonylfluoride), with five strokes of a motor-driven Potter-Elvehjem homogenizer (Bie and Berntsen, Rødovre, Denmark) at 1250 rpm. The homogenates were centrifuged in a Beckman L8 M centrifuge (Beckman Instruments Inc., Palo Alto, CA) at 4000 g for 15 min at 4°C. The supernatants were centrifuged at 200,000 g for 1 h. The resultant pellets were resuspended in dissecting buffer, and assayed for protein concentrations by using the method of Lowry.

Antibodies

Two polyclonal antibodies raised in rabbits were used in this study to label AQP1. The first, called anti-AQP1, was raised against purified human AQP1 isolated from red blood cells, and the second was raised against a peptide corresponding to the 10 amino-terminal amino acids of AQP1 (5,23). Both have previously been described for immunocytochemical analysis (5,17–19).

Electrophoresis and Immunoblotting

The membrane samples were solubilized in Laemmli sample buffer containing 2.5% sodium dodecyl sulfate (SDS). Samples were loaded at 10 μg/lane onto 12% SDS/polyacrylamide gel electrophoresis gels, run on a BioRad minigel system (BioRad, Hercules, CA), and proteins were transferred to nitrocellulose paper by electroelution. The blots were blocked for 1 h with 5% skimmed milk in phosphate-buffered saline-T (PBS-T; 80 mM Na_2HPO_4, 20 mM NaH_2PO_4, 100 mM NaCl, 0.1% Tween-20, pH 7.5), and then washed with PBS-T. The blots were then incubated overnight at 4°C with antibody in PBS-T with 0.1% BSA at the following dilutions: anti-AQP1 (0.01 μg immunoglobulin G [IgG]/mL) and affinity-purified anti-N peptide (5,18,23) (0.05 μg IgG/mL). After being washed, the blots were incubated for 1 h at room temperature with horseradish peroxidase-conjugated goat-anti-rabbit secondary antibody (P448; DAKO, Glostrup, Denmark; 1:3000). After the final washing, antibody binding was visualized using the ECL system (enhanced chemiluminescence; Amersham International, Little Chalfont, U.K.). Controls using affinity-purified antibody preadsorbed with excess purified AQP1, or omission of primary or secondary antibody, revealed no labeling.

Immunocytochemistry

Preparation of tissues for immunolocalization of AQP1. Surgical specimens of nonpathological human kidney tissue (from kidneys with tumors at the opposite pole) were fixed either by immersion fixation or by partial immersion fixation and partial simultaneous vascular perfusion of the excised kidney tissue with 8% paraformaldehyde in 0.1 M sodium cacodylate buffer, pH 7.2. Tissue blocks were prepared from outer cortex, outer and inner stripe of the outer medulla, and from different levels of the inner medulla. The blocks were postfixed in the same fixative for 2 h, infiltrated for 30 min with 2.3 M sucrose containing 2% paraformaldehyde, mounted on holders, and rapidly frozen in liquid nitrogen, essentially as described previously (17,18). The frozen tissue blocks were either cryosectioned for light microscope immunohistochemistry, or were freeze-substituted and embedded in Lowicryl for immunoelectron microscopy.

Freeze-substitution of kidney tissue. The frozen samples were freeze-substituted in a Reichert AFS (Reichert, Vienna, Austria) as described before (13,17). In brief, the samples were sequentially equilibrated over 3 days in methanol containing 0.5% uranyl acetate at temperatures gradually increasing from −85°C to −70°C, and then rinsed in pure methanol for 24 h while the temperature was increased from −70°C to −45°C. At −45°C, the samples were infiltrated with Lowicryl HM20 (Polysciences Ltd., Eppelheim, Germany) and methanol 1:1, 2:1 and, finally, pure Lowicryl HM20 before ultraviolet-polymerization for 2 days at −45°C and 2 days at 0°C.

Immunohistochemistry and immunoelectron microscopy. The use of anti-AQP1 antibodies for immunocytochemistry has been thoroughly described previously (17,18). Affinity-purified polyclonal anti-AQP1 recognizing the COOH terminal part of AQP1 was used at 0.1 to 0.2 μg/mL.

For light microscopical analysis, cryosections approximately 0.8 μm in thickness were obtained with a Reichert Ultracut S Cryoultramicrotome (Leica Aktiengesellschaft, Vienna, Austria) and were placed on gelatin-coated glass slides. After preincubation for 5 min with PBS containing 1% BSA and 0.05 M glycine, the sections were incubated overnight at 4°C with anti-AQP1 antibodies diluted in PBS with 0.1% BSA or 0.1% skimmed milk. The labeling was visualized by incubation for 1 h at room temperature with horseradish peroxidase–conjugated secondary antibody (P448, 1:100; DAKO, Glostrup, Denmark), followed by incubation with diaminobenzidine for 10 min. Sections were counterstained with Meier counter stain.

For electron microscopy, immunolabeling was performed on ultrathin Lowicryl HM20 sections (40 to 60 nm), which were incubated overnight at 4°C with anti-AQP1 diluted in PBS with 0.1% BSA or 0.1% skimmed milk. The labeling was visualized with goat-anti-rabbit

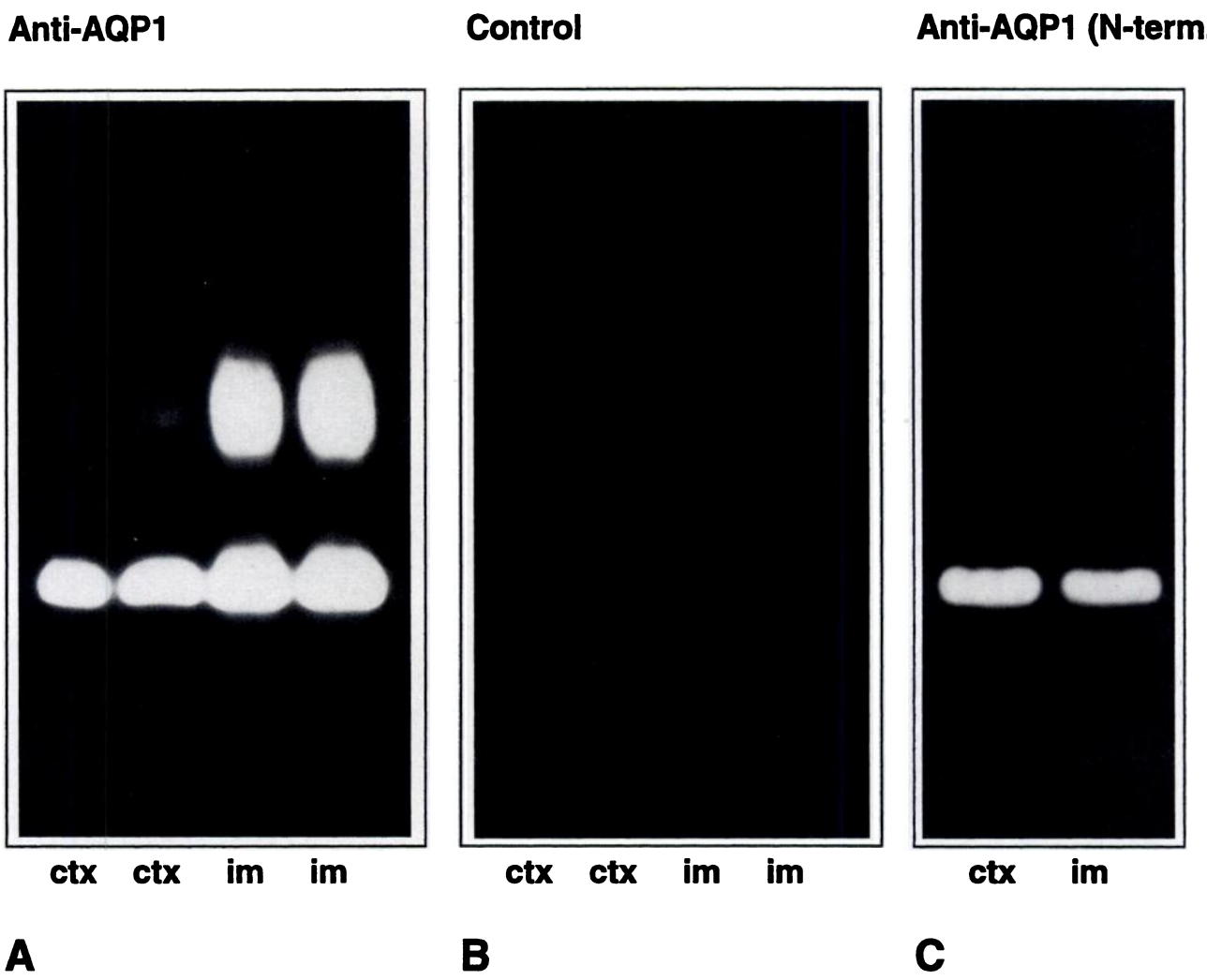

Figure 1. Immunoblots of membrane preparations from human kidney cortex and inner medulla. Samples were run on 12% polyacrylamide gels using sodium dodecyl sulfate-polyacrylamide gel electrophoresis. (A) Immunoblot of crude membrane fractions of kidney cortex (ctx, 10 μg/lane) and inner medulla (im, 20 μg/lane) labeled with affinity-purified anti-AQP1 antibody. A strong 28-kd band corresponding to nonglycosylated AQP1 is seen in both cortex and inner medulla. The 35- to 50-kd band, corresponding to the glycosylated species, is faintly visible in cortex but distinct in the inner medulla. (B) Negative control. Immunoblot of crude membrane from kidney cortex (10 μg/lane) was incubated with affinity-purified antibody previously reacted with purified AQP1. The signal is completely ablated. (C) Immunoblot of crude membrane fraction of kidney cortex (ctx, 10 μg/lane) and inner medulla (im, 10 μg/lane) labeled with affinity-purified antibody raised against a peptide corresponding to the ten N-terminal amino acids of AQP1. The 28-kd band corresponding to nonglycosylated AQP1 comigrates with the band seen in the left panel. The glycosylated band varied in intensity from preparation to preparation and was not visible in the exposure illustrated.

IgG conjugated to 10-nm colloidal gold particles (GAR.EM10; Bio-Cell Research Laboratories, Cardiff, UK) diluted 1:50 in PBS with 0.1% BSA or 0.1% skimmed milk. The sections were stained with uranyl acetate for 10 min before examination in a Philips 208, a Philips CM100 (both from Philips, Eindhoven, The Netherlands), or a Zeiss 912 Omega electron microscope (Zeiss, Oberkochen, Germany).

Immunolabeling controls. The following controls were performed at the light and electron microscopical levels: (*1*) The primary antibody was substituted with non-immune rabbit IgG prepared by protein-A-purification; (*2*) adsorption controls were made by incubation with affinity-purified anti-AQP1 (0.1 μg/mL) previously reacted with purified AQP1 (10 μg/mL); (*3*) incubation without use of primary antibody or without primary and secondary antibody. All controls revealed a complete absence of labeling.

In Situ *Hybridization*

In situ hybridization for AQP1 was performed as previously described (2). Fresh human kidneys were obtained from patients undergoing nephrectomy for renal tumors at the National Institutes of Health (NIH) Clinical Center. Patients gave informed consent to the disposition of their surgically removed tissues under a protocol approved by the NIH Clinical Center Institutional Review Board. Aside from the diagnosis of renal tumor, the patients were free of systemic or renal disease, including hypertension and diabetes, and were 43 to 48 yr of age. The half of the kidney appearing to be tumor-free was quickly cut into blocks and frozen over dry ice.

Frozen sections, 10-μm thick, were cut at −15°C, thaw-mounted on poly-L-lysine–coated slides, and stored at −70°C until hybridization. Tissue sections were prepared in the following manner: before

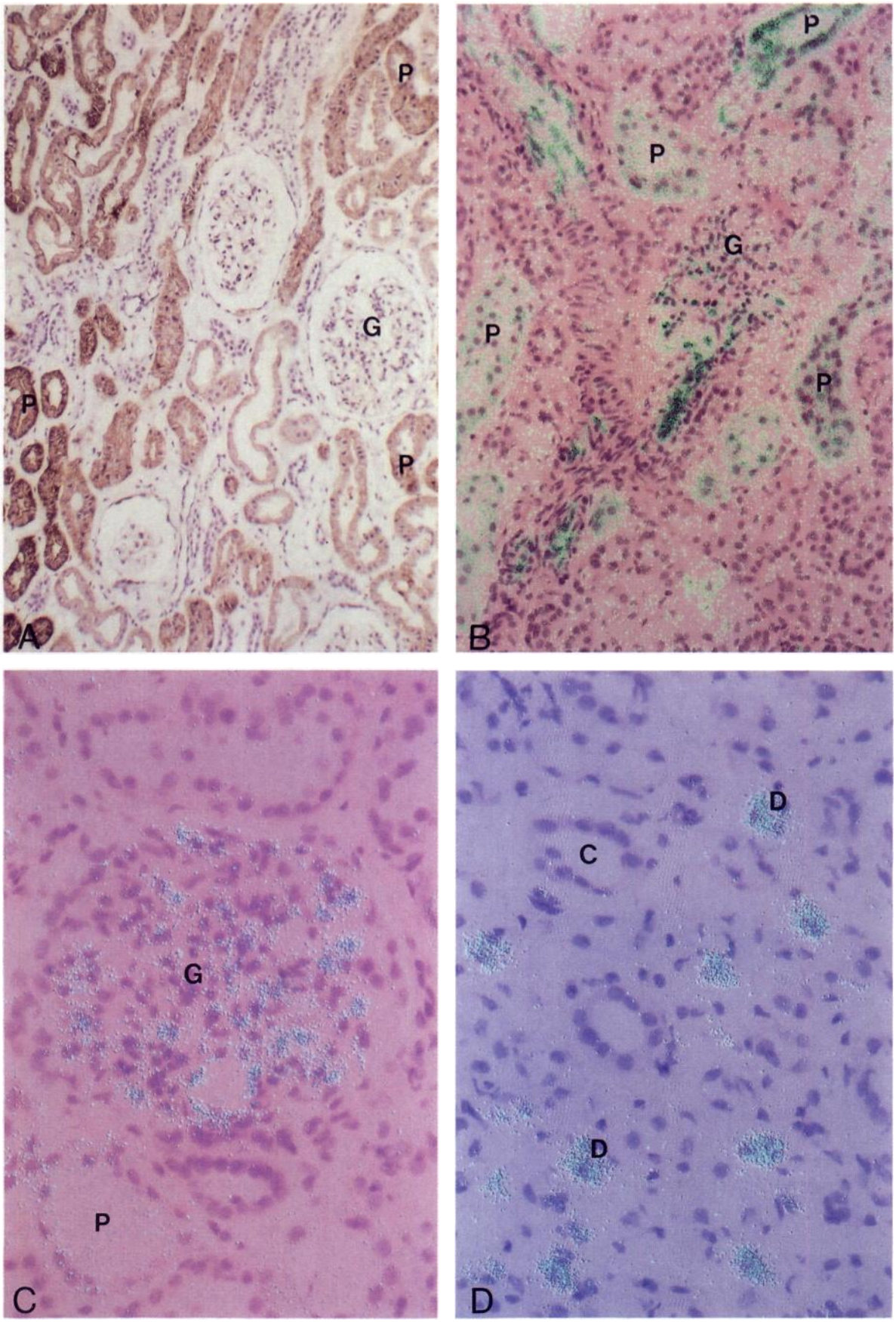

Figure 2. Immunocytochemical localization of AQP1 in thin cryosections (0.8 μm) of human kidney cortex (Panels A through D), outer medulla (Panels E through F), and inner medulla (Panels G through I). Sections were immunolabeled with affinity-purified anti-AQP1, and

hybridization, sections were warmed to 25°C, fixed in 10% formaldehyde and soaked for 10 min in 0.25% acetic anhydride/0.1 M triethanolamine hydrochloride/0.9% NaCl. The tissue was then dehydrated through an ethanol series, delipidated in chloroform, rehydrated, and air-dried.

An exonuclease III fragment corresponding to nucleotides +15 to +451 of the human CHIP28 (AQP1) cDNA was subcloned into pBluescript II (Stratagene, Inc., La Jolla, CA) for transcription of both antisense (using T7 RNA polymerase) or sense (using T3 RNA polymerase) ^{35}S-labeled cRNA probes.

The ^{35}S-labeled probes (107 dpm/mL or approximately 50 ng/mL) were added to hybridization buffer composed of 50% formamide, 0.3 M NaCl, 20 mM Tris HCl, pH 8, 5 mM EDTA, 500 μg tRNA, 10% dextran sulfate, 10 mM dithiothreitol, and 0.02% each of BSA, ficoll, and polyvinylpyrrolidone. After the ^{35}S-labeled probe in hybridization buffer was added to the sections, coverslips were placed over the sections and the slides were incubated in humidified chambers overnight (14 h) at 55°C. Slides were washed several times in 4X SSC (sodium chloride/sodium citrate) to remove cover slips and hybridization buffer, dehydrated, and immersed in 0.3 M NaCl, 50% formamide, 20 mM Tris HCl, and 1 mM EDTA at 60°C for 10 min. Sections were then treated with RNase A (20 μg/mL) for 30 min at room temperature, followed by a 15-min wash in 0.1X SSC at 55°C. Slides were air-dried and apposed to Hyperfilm-βMax (Amersham) and then dipped in Kodak NTB2 nuclear emulsion (Eastman Kodak, Rochester, NY), stored with desiccant at 4°C, developed, and counterstained with Meier's hematoxylin and eosin for microscopic evaluation.

Results

Immunoblotting of Human Kidney Membrane Fractions Using Anti-AQP1 Antibodies

Immunoblotting using crude membrane fractions of human kidney cortex (Figure 1) demonstrated the 28-kd and the 35- to 50-kd bands, corresponding to nonglycosylated and glycosylated AQP1, as previously shown in human red blood cells as well as kidney and other tissues from rat (5,18). The 35- to 50-kd had a weaker appearance in cortex, compared with inner medulla (Figure 1A). Both the antibody raised against highly purified human AQP1 from red blood cells and the one raised against a peptide corresponding to the 10 N-terminal amino acids of AQP1 labeled bands that comigrated, confirming the selectivity of labeling (Figure 1C). Immunolabeling controls were negative (Figure 1B). Immunoblots using membrane fractions from outer (not shown) and inner medulla (Figure 1A) gave similar labeling patterns.

Immunocytochemical Localization of AQP1 in Semi-Thin Cryosections of Human Kidney

Detailed immunolocalization of AQP1 was performed on semithin cryosections from different regions of the human kidney (Figure 2). In the glomerulus, immunoperoxidase labeling revealed the presence of AQP1 in the endothelium of glomerular capillaries (Figure 2A). In contrast, podocytes were unlabeled. Labeling for AQP1 was also present in mesangial regions and was associated with mesangial cells. Epithelial cells of Bowman's capsule showed no labeling, except where it was continuous with the very beginning of the proximal tubule. Immunolabeling controls performed with affinity-purified antibody previously preadsorbed with excess purified AQP1 showed a complete absence of labeling (Figure 2B).

Proximal tubules revealed strong staining of the brush border and basolateral plasma membranes (Figure 2C) consistent with the labeling pattern in rat (17,18), except that in some nephrons weak labeling was present in the initial part of the proximal tubule (arrow in Figure 2D). Pronounced differences in the intensities of labeling between different cross-sections of proximal tubules were apparent. Straight proximal tubules generally exhibited the most intense labeling but marked differences were also encountered between different parts of the convoluted proximal tubule (see the Discussion section).

Descending thin limbs labeled distinctly for AQP1 in the inner stripe of the outer medulla (Figure 2E). In regions with vascular bundles, several thin-walled thin limb structures were labeled corresponding to descending thin limbs of short loops (Figure 2E). Furthermore, in the periphery of the bundles, tubules with tall epithelial cells were extensively labeled. On the basis of their location in relation to the bundles, their cell height, and their multiple, dilated intercellular spaces and luminal cell-to-cell contacts, they were identified as descending thin limbs of long loops (9). In contrast, thick ascending limbs

labeling was visualized with peroxidase-conjugated secondary antibody. (A) Glomerular capillaries exhibit significant labeling (arrowheads), whereas podocytes are completely unlabeled. Mesangial regions (asterisks) exhibit weak labeling. The capsule of Bowman is unlabeled except for minor areas (upper left) that presumably correspond to regions forming the neck of the proximal tubule. Proximal tubules also exhibit extensive labeling, whereas distal tubules are unlabeled. (B) Immunolabeling control. Use of affinity-purified antibody previously reacted with purified AQP1 reveals absence of labeling. (C) Convoluted proximal tubules display marked labeling of both brush border and basolateral plasma membrane foldings. (D) In some nephrons, the initial part of the proximal tubule (arrow) exhibits significant labeling, although generally it is substantially weaker than in more distal segments. Peritubular capillaries are also labeled (arrowheads). (E) Section from outer medulla, revealing extensive labeling of thin limb segments. Most are thin-walled segments, whereas others display a characteristic thick-walled structure with labeling of both apical and basolateral domains (asterisk), interpreted as a descending thin limb of a long loop nephron. (F) Section from the junction between outer and inner medulla. In the periphery of the vascular bundles, several thin limbs with characteristic thick walls with distended intercellular spaces are seen to be heavily labeled. These were interpreted as descending thin limbs. Collecting ducts and distal tubules are unlabeled (asterisks). (G) Section from kidney inner medulla. Strong labeling is seen of structures interpreted as thin descending limbs of the loop of Henle. Notice the abrupt transition from immunoreactive to immunonegative cells (arrows). Also note that some thin limbs are unlabeled. These were interpreted as ascending thin limbs. (H) Strong labeling of some thin limbs is seen, whereas other thin limb structures are completely unlabeled. A very faint labeling is observed on the luminal surface of the collecting duct cells (arrowheads). (I) Immunolabeling control. Use of affinity-purified antibody previously reacted with purified AQP1 reveals absence of labeling. (Original magnification, ×800).

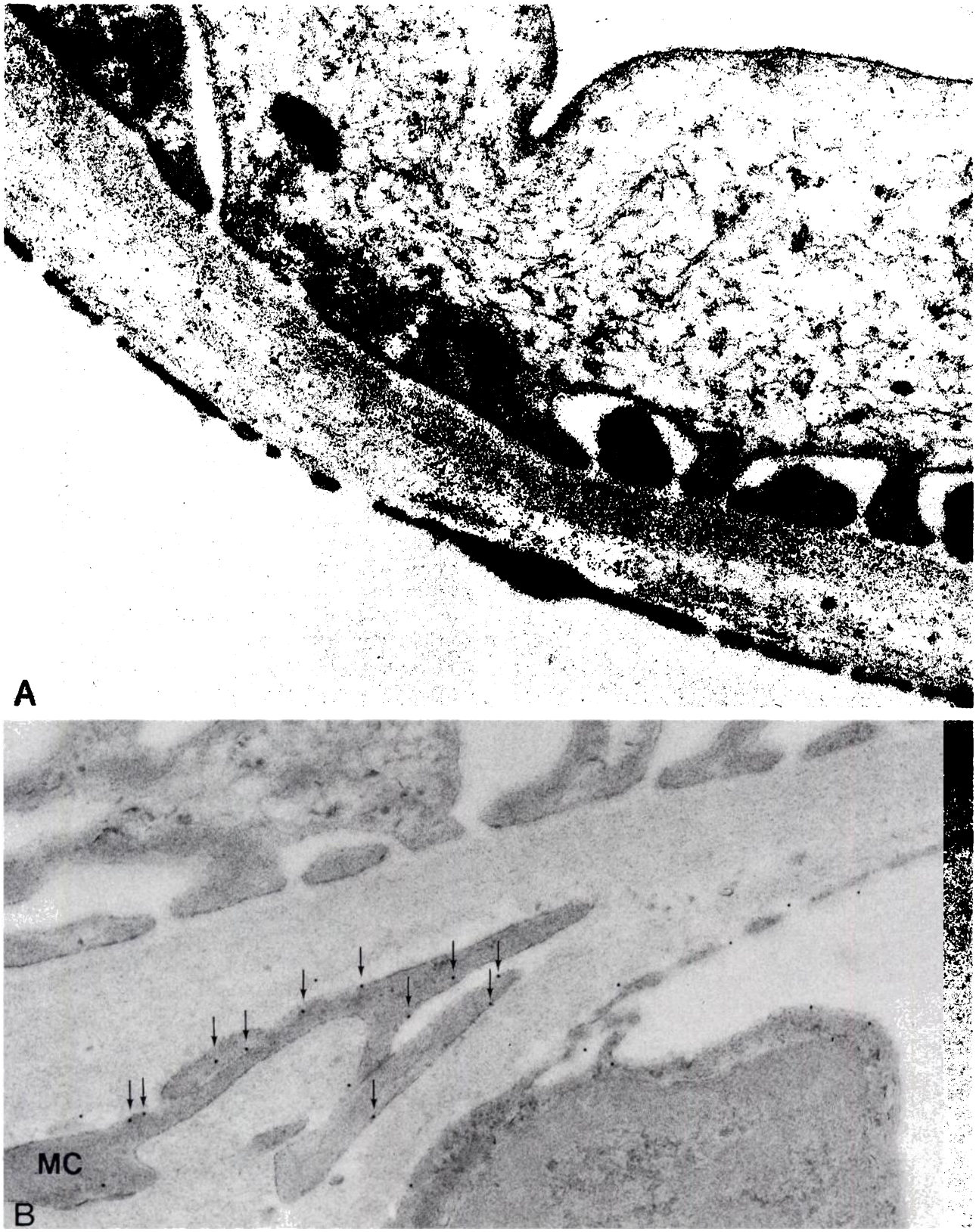

Figure 3. (A) Immunoelectron microscopic labeling of AQP1 in glomerulus. AQP1 is present in the endothelium of the glomerular membrane, but not associated with the foot processes of the epithelial cells. Notice that both the luminal and the abluminal plasma membranes of the endothelial cell are labeled, whereas the endothelial fenestrae display little or no labeling. (B) Anti-AQP1 labels mesangial cell membranes (arrows) in the glomerulus (MC). Podocyte processes are unlabeled, whereas one endothelial cell displays labeling. (Original magnification, ×60,000).

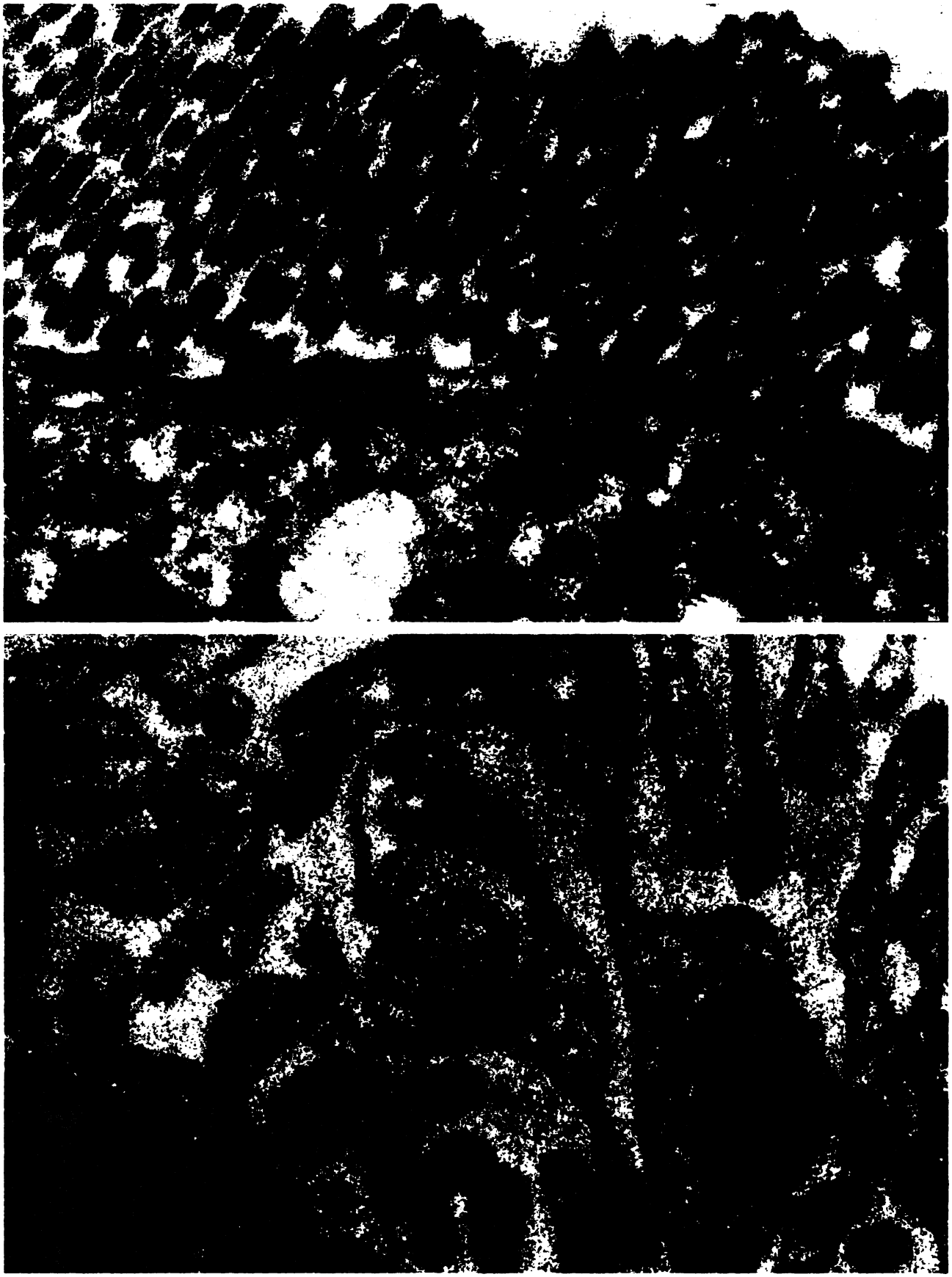

Figure 4. (A) Immunoelectron microscopic labeling of AQP1 in proximal tubule. Anti-AQP1 labels the microvilli of the brush border, whereas only a few endocytic vesicles are labeled. (Original magnification, ×60,000). (B) Basolateral membranes of proximal tubule are uniformly labeled. BM, basement membrane. (Original magnification, ×60,000).

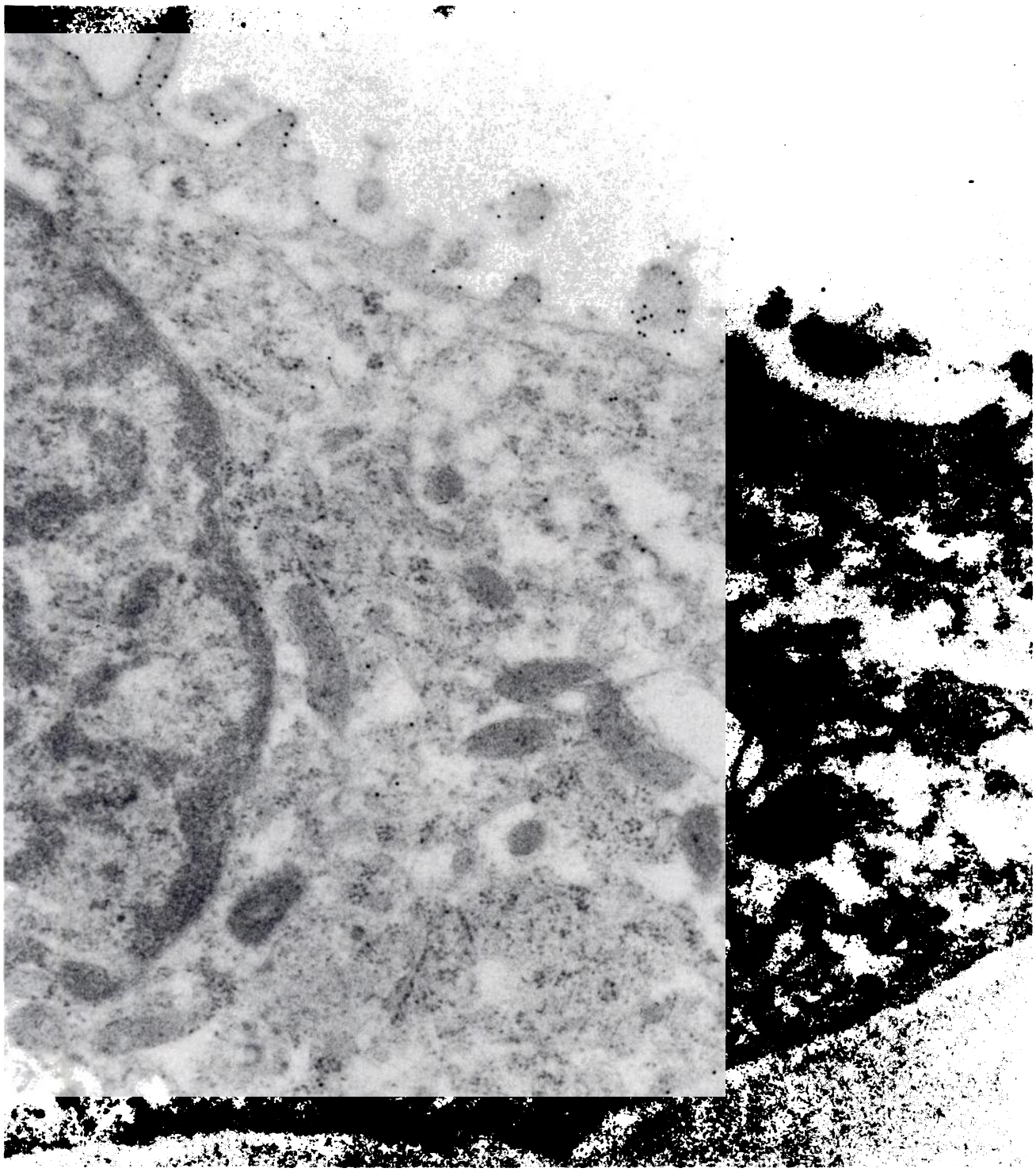

Figure 5. Anti-AQP1 labeling of epithelial cell of a descending thin limb in the inner stripe of the outer medulla. This thick-walled nephron segment, with characteristic small microvilli, represents a descending thin limb, presumably of a long nephron. Both cell surfaces, including the microvilli, are labeled. (Original magnification, ×60,000).

were unlabeled. In the inner medulla, strong labeling was seen in cross-sections of tubules with low epithelium, which typically had dilated intercellular spaces (Figure 2F). These tubule segments were identified as the inner medullary part of the descending thin limbs. Tubules of comparable structure, but typically without dilated intercellular spaces, were unlabeled (Figure 2G) and interpreted as cross-sections of ascending thin limbs. In addition, there were tubular profiles with an abrupt transition from labeled to unlabeled cells (arrows in Figure 2G) consistent with the transition between descending and ascending thin limb epithelium. Collecting duct cells were generally unlabeled, except that a very faint reaction was present on the luminal surface of some tubule cells (arrowheads in Figure 2H). Although crossreactivity with AQP2 in the collecting duct

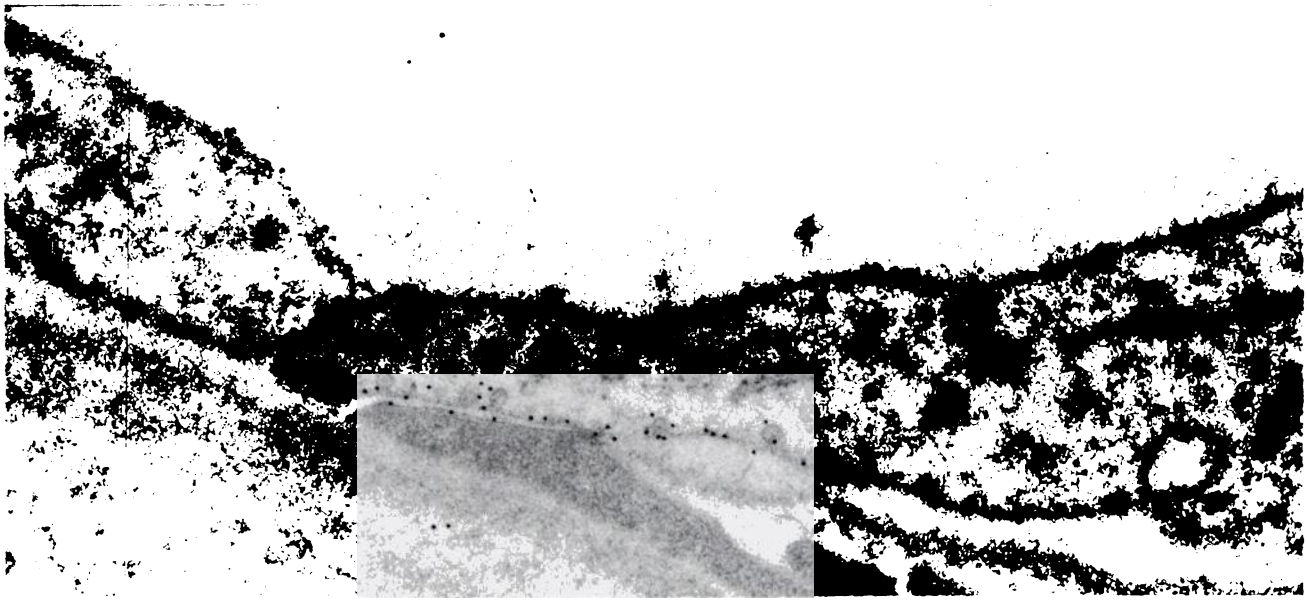

Figure 6. Anti-AQP1 labeling of cells in descending thin limb of inner medulla. The cells exhibit strong labeling of both apical and basal plasma membranes. Adjacent interstitial cells are unlabeled. (Original magnification, ×60,000).

cannot be excluded, this very faint staining might represent an artifact. Immunolabeling controls from outer medulla (not shown) as well as inner medulla (Figure 2I) were completely negative.

Immunoelectron Microscopical Localization of AQP1 in the Glomerulus

In contrast to the rat glomerulus (18,22), endothelial cells in the human glomerulus exhibited extensive AQP1-immunolabeling in ultrathin Lowicryl sections (Figure 3A). The labeling was associated both with the luminal and abluminal cell membranes, which appeared equally labeled (Figure 3A). The labeling was predominantly associated with the nonfenestrated plasma membrane regions, including that part covering the cell body with the nucleus, whereas fenestrae showed no distinct labeling. In contrast to the extensive labeling of the endothelium, glomerular podocytes were unlabeled. Mesangial cells, including their long projections, also showed plasma-membrane labeling (Figure 3B), although generally less intense than the labeling of the endothelial cell membranes (Figures 2 and 3).

Immunoelectron Microscopical Localization of AQP1 in Tubules

Proximal tubules in human kidneys showed distinct labeling of both the apical and the basolateral plasma membranes (Figure 4), but the labeling density varied between different proximal tubule cross-sections as observed by light microscope immunocytochemistry. The labeling was associated with the microvilli of the brush border and the labeling density was similar along the length of the microvilli. Endocytic invaginations and vesicles were less heavily labeled or unlabeled (Figure 4A). Both the lateral and basal domains of the basolateral plasma membrane were labeled (Figure 4B), and the labeling extended all the way to the junctional complex. Thus, the labeling pattern of individual cells was very similar to that observed in the rat (17).

Ultrathin Lowicryl sections of tubules in the inner stripe of the outer medulla displaying the characteristic tall cells (seen in Figure 2F) revealed intense labeling of apical and basolateral plasma membranes (Figure 5). These tubules displayed ultrastructural characteristics of descending thin limbs of long loops in rat outer medulla, further substantiating that these tubules corresponded to the descending thin limb. The thin-walled tubules seen in Figure 2E also displayed significant labeling and a simplified ultrastructure similar to the descending thin limb of short loops in the rat (not shown). In the inner medulla, labeled tubules with thin epithelium (Figure 2G and H) were similar in ultrastructure to tubules identified as descending thin limbs by Bulger *et al.* (4). They showed an extensive gold labeling of both the luminal and abluminal plasma membranes (Figure 6A and B). Occasional cytoplasmic vesicles were also labeled (Figure 6A). The ultrastructural characteristics of the labeled tubules were also similar to the descending thin limbs in the rat inner medulla, further supporting their identity as descending thin limbs.

Immunolabeling performed with the anti-N-peptide antibody gave labeling similar to that seen with the anti-AQP1 (raised against the purified AQP1 protein), although the labeling intensity was much weaker (not shown).

Immunoelectron Microscopical Localization of AQP1 in Capillary Endothelium

In the peritubular and periglomerular interstitium in cortex, the endothelium of the fenestrated capillaries showed marked AQP1-immunolabeling (Figure 7). Higher magnifications revealed labeling of both luminal and abluminal plasma membrane domains (Figure 7B). Capillary endothelium in outer medulla (Figure 8) and inner medulla (not shown) also dis-

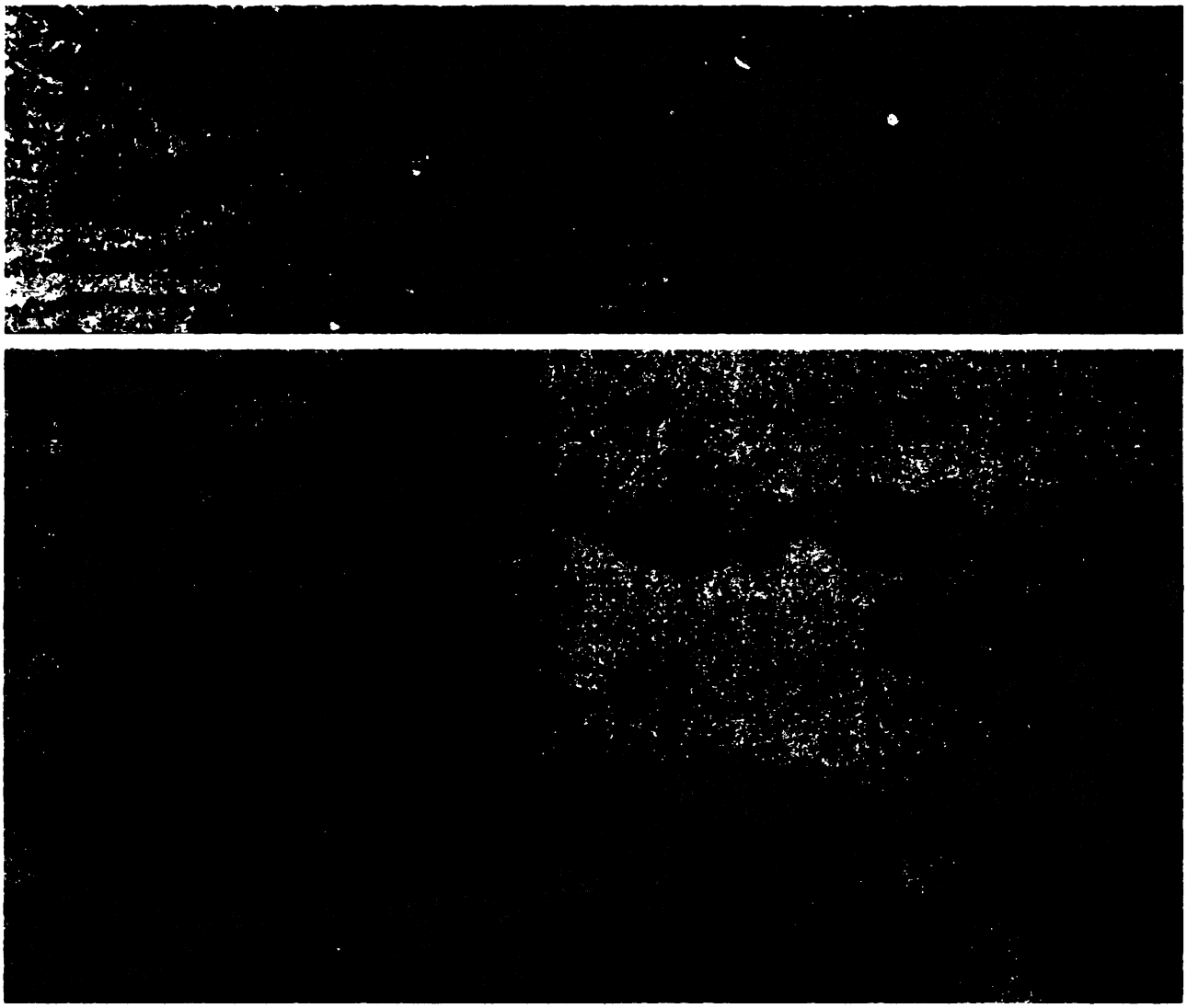

Figure 7. Anti-AQP1 labeling of peritubular capillary endothelium. (A) Low magnification showing capillary adjacent to proximal tubule (PT). (Original magnification, ×15,000). (B) Higher magnification of area shown above (asterisk in Panel A) shows intense AQP1 labeling of luminal and abluminal membranes of the fenestrated endothelium. (Original magnification, ×60,000).

played significant labeling. The labeling density of the endothelium appeared to be similar in cortical and outer and inner medullary capillaries (Figure 7 and 8). In addition to the labeling of the plasma membranes, vesicular profiles in the cytoplasm of the endothelial cells were also labeled (arrowheads in Figure 8).

Segmental Differences in AQP1 Expression in Proximal Tubule

As shown in Figure 2, proximal tubules exhibited differences in labeling intensity, as observed in semi-thin cryosections. The extent of this difference was further analyzed by immunolabeling of survey paraffin sections (Figure 9A). These sections revealed a marked difference in labeling intensity between cross-sectioned proximal tubules, with some displaying very intense labeling and again others displaying little or even no labeling (Figure 9A). The glomerulus also showed a distinct labeling, confirming the observations shown in Figure 2.

Distribution of AQP1 mRNA Revealed by In Situ *Hybridization*

The distribution of AQP1 mRNA was analyzed by *in situ* hybridization in frozen sections of cortex and outer and inner medulla. In cortex, the proximal tubules exhibited significant signals, but with varying intensity. Some tubules revealed very strong signals (Figure 9B and C), whereas others showed low or virtually no signals. Thus, both the *in situ* hybridization and immunolabeling documented extensive differences in AQP1 expression within different segments of the proximal tubule.

Furthermore, strong signals were observed in positively identified glomeruli (Figure 9B and C). Higher magnification of the glomerular region (Figure 9C) showed the signals associated with the capillary loops and (to some extent) mesangial regions, whereas no detectable signals were associated with Bowman's capsule. In the inner medulla (Figure 9D), thin limb structures were either very intensely labeled or unlabeled. The labeled thin limbs, on the basis of their distribution in cross-sections, presumably corresponded to descending thin limbs

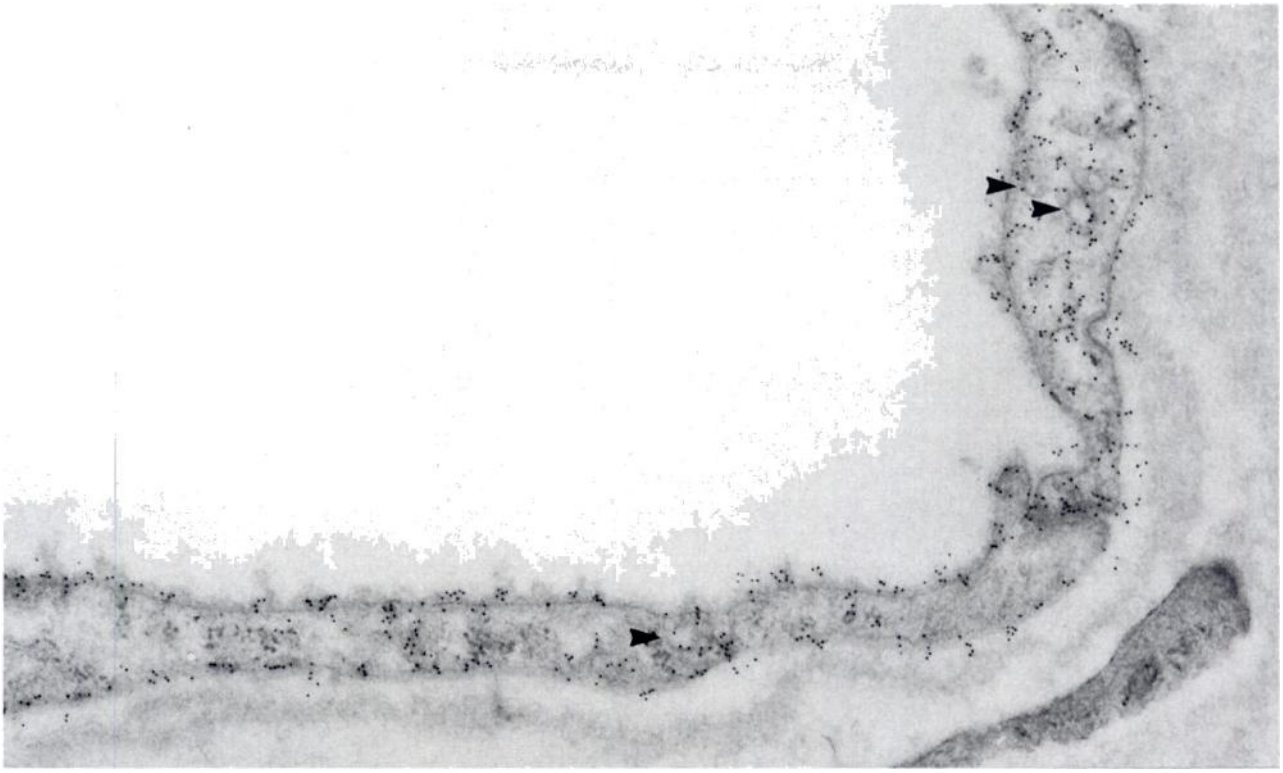

Figure 8. Anti-AQP1 labeling of endothelial cells (in other regions showing fenestrae) in the inner stripe of the outer medulla. Both cell surfaces are labeled, as well as some internal vesicular and tubular profiles (arrowheads). (Original magnification, ×60,000.)

and the unlabeled to ascending thin limbs, respectively. Collecting ducts and thick ascending limbs showed no signals whereas detectable signals were seen in regions containing capillaries. Thus, the *in situ* hybridization revealed exactly the same general expression pattern as did immunocytochemical analysis at the light and electron microscopical levels.

Discussion

Expression of AQP1 in the Human Proximal Tubule

The AQP1 expression pattern in the human kidney is similar to that observed in the rat kidney, but with some notable differences. The study presented here demonstrates that AQP1 water channel protein is expressed heavily in the human proximal tubule, consistent with initial studies (5). Labeling was found both in proximal convoluted tubules and in proximal straight tubules, segments that exhibit distinctly different ultrastructural features (24). An important observation is the uneven distribution of AQP1 along the human proximal tubule, extending initial observations (5). The expression is most intense in the pars recta, with low levels in the initial portions of some, but not all, proximal tubules. The striking difference in levels of expression was observed both by immunohistochemistry and immunocytochemistry at the light and electron microscopical level and, in addition, by *in situ* hybridization. Because functional studies in the rat kidney (11) have revealed an equally high water permeability in the initial and later segments of the proximal tubule, the absence or reduction in AQP1 expression in some part of the human proximal tubule is notable. Because such tubules, examined both by immunocytochemistry and by *in situ* hybridization, were localized adjacent to tubules displaying very high levels of AQP1 protein or mRNA, it is highly unlikely that the differences in the labeling occur because of methodological factors. Instead it is a possibility that another aquaporin homologue may be expressed in these segments without or with very low levels of AQP1 protein and mRNA, *i.e.*, the initial portion of the proximal tubule. It may be speculated that this possibility is consistent with the recent report of a few individuals with low or zero expression of AQP1 who did not show any apparent polyuria or impairment of renal function (21). It should, however, be pointed out that the absence of AQP1 may not necessarily lead to major concentrating defects, because this could theoretically be overcome by establishing a slightly higher gradient across the proximal tubule and descending thin limbs to drive water reabsorption across the epithelial plasma membranes. This would represent an energetically unfavorable situation, but would allow water to be reabsorbed.

Expression of AQP1 in the Thin Limb Epithelia

Immunocytochemistry and *in situ* hybridization revealed a very intense labeling of some thin limbs in the human kidney, whereas others were unlabeled. This is similar to the abundant AQP1 labeling of rat and chinchilla descending thin limb epithelium and absence of AQP1 labeling in ascending thin limbs (17,18). As in the rat, there was an abrupt transition from strongly labeled thin limb epithelial cells to unlabeled cells. However, in contrast to the situation in the rat, in which descending thin limb epithelium (short and long loops) display marked ultrastructural differences from ascending thin limb epithelium (9), thin limb epithelium in the human kidney has a

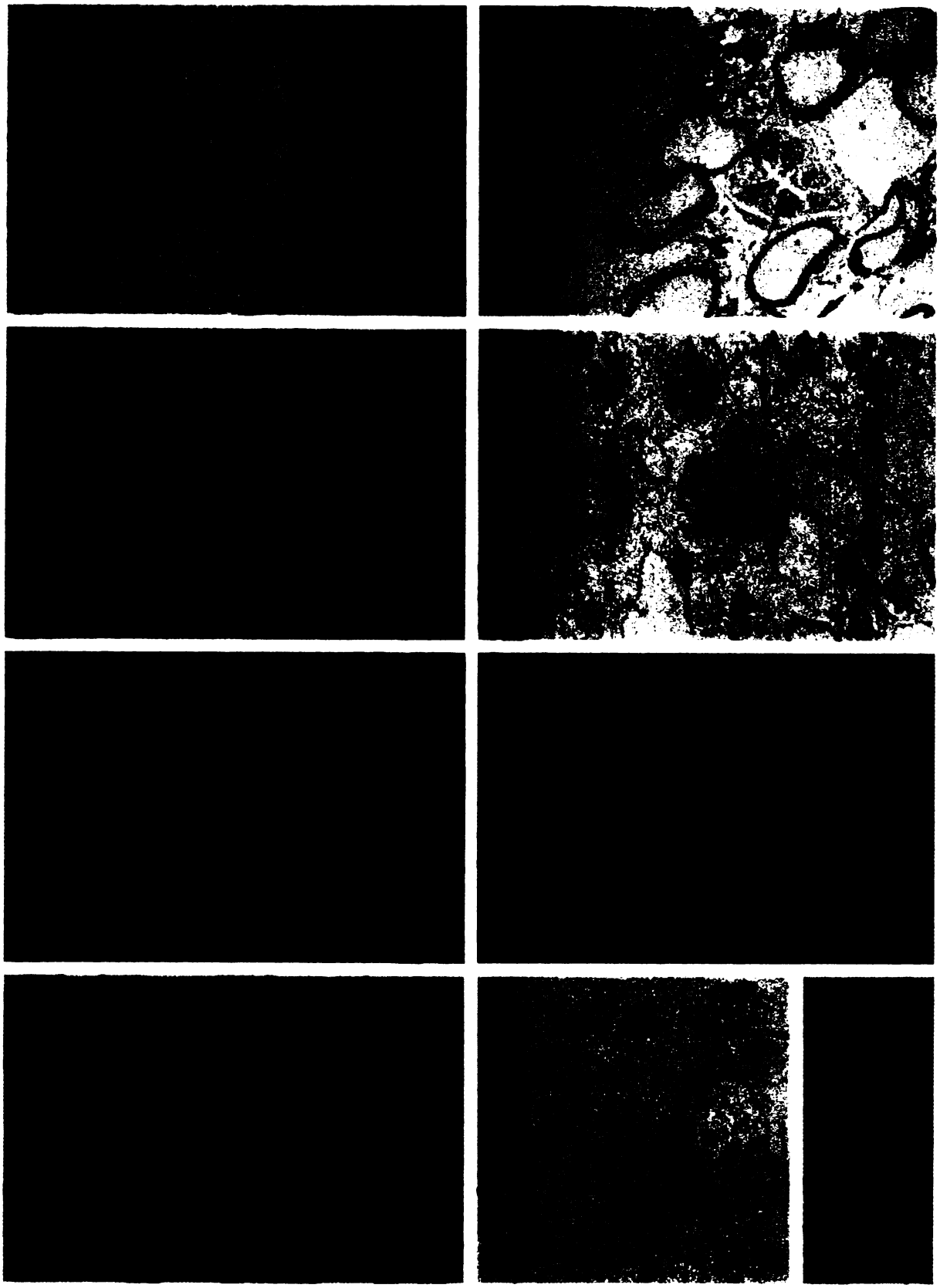

Figure 9. AQP1 expression in human kidney demonstrated by immunohistochemistry in survey paraffin sections (Panel A) and by *in situ* hybridization in unfixed frozen cryostat sections (Panels B through D). (A) AQP1 labeling varies greatly between different proximal tubule cross-sections (P), some being extensively stained whereas others are unstained or only weakly stained. Glomeruli (G) are weakly stained.

much less complex ultrastructure (4). The distinct labeling pattern with labeled and unlabeled thin limbs suggests that the structural organization of the thin limbs share both functional and structural similarities with the rodent kidneys most often used for physiological and pathophysiological experiments. Moreover, AQP1 may represent a marker for descending thin limbs and help distinguish those from the ultrastructurally very similar ascending thin limbs in the human kidney.

Localization of AQP1 in Human Glomerulus

In the rat glomerulus, anti-AQP1 did not label any of the cell types (18). However, in the human glomerulus, distinct AQP1 protein and mRNA were demonstrated by immunocytochemistry and *in situ* hybridization, respectively. Immunoelectron microscopy revealed labeling of the endothelium, on both the luminal and abluminal plasma membranes.

The glomerular filtration barrier consists of capillary endothelium, basement membrane, and glomerular epithelial cells (podocytes). It has generally been believed that in the endothelium, water and solute transport occurs via the fenestrae. The observations from this study suggest that this view may have to be modified, and that water transport may also cross the endothelium via a transcellular route, *i.e.*, mediated via AQP1 water channels in the luminal and abluminal plasma membranes.

Within the glomerulus, mesangial cells also exhibit distinct immunoreactivity, thus providing further evidence for their ontogenic relationship to endothelial cells. The presence of aquaporin in the mesangial cell plasma membranes suggests that these cells have the capacity to change their volume rapidly during physiological or pathological conditions, consistent with other ultrastructural characteristics of the mesangial cells, including their well-developed cytoskeleton. Indeed it has been pointed out that mesangial cells seem to swell more readily than endothelial cells in human and experimentally induced disease, and that swollen mesangial cells, together with swollen endothelial cells, may account for much of the ischemia seen in many glomerular diseases (10).

Peritubular Capillaries Express AQP1

In kidney cortex and medulla, fenestrated peritubular capillaries showed strong labeling for AQP1.This finding is consistent with recent preliminary evidence that AQP1 is also expressed in fenestrated capillaries outside the kidney (*e.g.*, human thyroid and pancreas; Elkjaer, Marples, Maunsbach, Agre and Nielsen, unpublished observations). The localization of AQP1 in fenestrated capillaries is different from rat kidney, in which virtually no labeling was associated with peritubular capillaries. This may reflect absence of AQP1, or the presence only of levels that are below the detection limit, in rat fenestrated capillaries. However, the nonfenesterated capillary endothelium in rat kidney and extrarenal organs express AQP1 (19). Although functional studies (17) have documented $HgCl_2$ inhibition of water transport in isolated perfused descending vasa recta (nonfenestrated endothelium), the physiological role of aquaporins in transendothelial water transport in capillaries and venules remains unknown.

Conclusions

This study demonstrates that AQP1 is present in all proximal tubule segments, including segment 1 and the neck region. However, there are pronounced differences in expression levels with respect to both protein and mRNA levels, raising the possibility that additional aquaporin(s) may be present, notably in the initial part of the proximal tubule. AQP1 labeling continues directly from proximal tubules to descending thin limbs with a distinct transition from labeled to unlabeled thin limb epithelium, suggesting an abrupt transition between water-permeable descending thin limb and water-impermeable ascending thin limb in human kidney. AQP1 labeling is also observed in the endothelium of fenestrated glomerular capillaries, as well as fenestrated peritubular capillaries, suggesting the existence of a putative additional water conductive pathway in the glomerular filtration barrier.

Acknowledgments

The authors thank Else-Merete Løcke, Karen Thomsen, Trine Møller, and Mette Vistisen for excellent technical assistance. The authors thank Peter Ottosen, Erik Ilsø Christensen, and Klaus Borre for support in obtaining surgical human kidney specimens and for their helpful suggestions. Support for this study was provided by the Danish Medical Research Council, the Novo Nordisk Foundation, the Danish Research Academy, the Karen Elise Jensen Foundation, the Biomembrane Research Center at the University of Aarhus, the University of Aarhus Research Foundation, the Danish Foundation for the Advancement of Medical Science, the University of Aarhus, and grants from the National Institutes of Health.

References

1. Agre P, Brown D, Nielsen S: Aquaporin water channels: Unanswered questions and unresolved controversies. *Curr Opin Cell Biol* 7: 472–483, 1995
2. Bondy C, Chin E, Smith BL, Preston GM, Agre P: Developmental gene expression and tissue distribution of the CHIP28 water-channel protein. *Proc Natl Acad Sci USA* 90: 4500–4504, 1993
3. Brown D, Verbavatz JM, Valenti G, Lui B, Sabolic I: Localization of the CHIP28 water channel in reabsorptive segments of the rat male reproductive tract. *Eur J Cell Biol* 61: 264–273, 1993
4. Bulger RE, Tisher CC, Myers CE, Trump BF: Human renal

(Original magnification, ×100.) (B) Strong *in situ* hybridization signals (green dots represent photographic grains) are found to be associated with the glomerulus (G) and proximal tubules (P). Note that the signals of the proximal tubules vary substantially in intensity. (Original magnification, ×250.) (C) Higher magnification of *in situ* hybridization of glomerulus (G) and adjacent proximal tubules (P). Strong signals (turquoise dots represent photographic grains) are seen over glomerular capillaries as well as mesangial regions. (Original magnification, ×400.) (D) In a section from inner medulla, strong signals are seen associated with thin limbs (D), presumably descending thin limbs. C, collecting duct. (Original magnification, ×400.)

ultrastructure: II—The thin limb of Henle's loop and the interstitium in healthy individuals. *Lab Invest* 16: 124–141, 1967
5. Denker BM, Smith BL, Kuhajda FP, Agre P: Identification, purification, and partial characterization of a novel Mr 28,000 integral membrane protein from erythrocytes and renal tubules. *J Biol Chem* 263: 15634–15642, 1988
6. Kanno K, Sasaki S, Hirata Y, Ishikawa S-E, Fushimi K, Nakanishi S, Bichet DG, Marumo F: Urinary excretion of aquaporin-2 in patients with diabetes insipidus. *N Engl J Med* 332: 1540–1545, 1995
7. Knepper MA: The aquaporin family of molecular water channels. *Proc Natl Acad Sci USA* 91: 6255–6258, 1994
8. Knoers NVAM, van Os CH: The clinical importance of the urinary excretion of aquaporin-2. *N Engl J Med* 332: 1575–1576, 1995
9. Kriz W, Kaissling B: Structural organization of the mammalian kidney. In: *The Kidney: Physiology and Pathophysiology*, edited by Seldin DW, Giebisch G, New York, Raven Press, 1992, p 707
10. Latta H: Ultrastructure of the glomerulus and juxtaglomerulus apparatus. In: *Handbook of Physiology: Renal Physiology*, edited by Orloff J, Berliner RW, Baltimore, Waverly Press, Inc., 1973, pp 1–29
11. Liu FY, Cogan MG, Rector FCJ: Axial heterogeneity in the rat proximal convoluted tubule. II. Osmolality and osmotic water permeability. *Am J Physiol* 247: F822–F826, 1984
12. Maunsbach AB: The tubule. In: *Electron Microscopy in Human Medicine, Urogenital System and Breast*, Vol. 9, edited by Johannesen JV, London, McGraw Hill Book Company, 1979, pp 143–165
13. Maunsbach AB: Embedding of cells and tissues for ultrastructural and immunocytochemical analysis. In: *Cell Biology: A Laboratory Handbook*, edited by Celis JE, Orlando, Academic Press, 1994, pp 117–125
14. Maunsbach AB, Christensen EI: Functional ultrastructure of the proximal tubule. In: *Handbook of Physiology—Renal Physiology*, Vol. 1, edited by Windhager EE, New York, Oxford University Press, 1992, pp 41–107
15. Myers CE, Bulger RE, Tisher CC, Trump BF: Human renal ultrastructure. IV. Collecting duct of healthy individuals. *Lab Invest* 16: 655–668, 1966
16. Nielsen S, Agre P: The aquaporin family of water channels in kidney. *Kidney Int* 48: 1057–1068, 1995
17. Nielsen S, Pallone TL, Smith BL, Christensen EI, Agre P, Maunsbach AB: Aquaporin-1 water channels in short and long loop descending thin limbs and in descending vasa recta in rat kidney. *Am J Physiol* 268: F1023–F1037, 1995
18. Nielsen S, Smith B, Christensen EI, Knepper MA, Agre P: CHIP28 water channels are localized in constitutively water-permeable segments of the nephron. *J Cell Biol* 120: 371–383, 1993
19. Nielsen S, Smith BL, Christensen EI, Agre P: Distribution of aquaporin CHIP in secretory and resorptive epithelia and capillary endothelia. *Proc Natl Acad Sci USA* 90: 7275–7279, 1993
20. Preston GM, Carroll TP, Guggino WB, Agre P: Appearance of water channels in *Xenopus* oocytes expressing red cell CHIP28 protein. *Science* 256: 385–387, 1992
21. Preston GM, Smith BL, Zeidel ML, Moulds JJ, Agre P: Mutations in aquaporin-1 in phenotypically normal humans without functional CHIP water channels. *Science* 265: 1585–1587, 1994
22. Sabolic I, Valenti G, Verbavatz JM, Van Hoek AN, Verkman AS, Ausiello DA, Brown D: Localization of the CHIP28 water channel in rat kidney. *Am J Physiol* 263: C1225–C1233, 1992
23. Smith BL, Agre P: Erythrocyte Mr 28,000 transmembrane protein exists as a multisubunit oligomer similar to channel proteins. *J Biol Chem* 266: 6407–6415, 1991
24. Tisher CC, Bulger RE, Trump BF: Human renal ultrastructure. I. Proximal tubule of healthy individuals. *Lab Invest* 15: 1357–1394, 1966
25. Tisher CC, Bulger RE, Trump BF: Human renal ultrastructure. III. The distal tubule in healthy individuals. *Lab Invest* 18: 655–668, 1968
26. Tisher CC, Madsen KM: Anatomy of the kidney. In: *The Kidney*, edited by Brenner BM, Rector FC, Philadelphia, W.B. Saunders Company, 1991, pp 3–75
27. Zeidel ML, Ambudkar SV, Smith BL, Agre P: Reconstitution of functional water channels in liposomes containing purified red cell CHIP28 protein. *Biochemistry* 31: 7436–7440, 1992